Available online at www.sciencedirect.com
ScienceDirect
Journal of Crystal Growth 310 (2008) 110–115
JOURNAL OF CRYSTAL GROWTH
www.elsevier.com/locate/jcrysgro

Crystallization mechanisms of acicular crystals

François Puel[a], Elodie Verdurand[a], Pascal Taulelle[b], Christine Bebon[a], Didier Colson[a], Jean-Paul Klein[a], Stéphane Veesler[b,*]

[a]*LAGEP, UMR CNRS 5007, Université Lyon 1, CPE Lyon, Bât. 308G, 43 Bd du 11 novembre 1918, F-69622 Villeurbanne Cedex, France*
[b]*Centre de Recherche en Matière Condensée et Nanosciences (CRMCN)[1]—CNRS, Campus de Luminy, Case 913, F-13288 Marseille Cedex 09, France*

Received 10 September 2007; accepted 3 October 2007
Communicated by K. Sato
Available online 9 October 2007

Abstract

In this contribution, we present an experimental investigation of the growth of four different organic molecules produced at industrial scale with a view to understand the crystallization mechanism of acicular or needle-like crystals. For all organic crystals studied in this article, layer-by-layer growth of the lateral faces is very slow and clear, as soon as the supersaturation is high enough, there is competition between growth and surface-activated secondary nucleation. This gives rise to pseudo-twinned crystals composed of several needle individuals aligned along a crystallographic axis; this is explained by regular over- and inter-growths as in the case of twinning. And when supersaturation is even higher, nucleation is fast and random.

In an industrial continuous crystallization, the rapid growth of needle-like crystals is to be avoided as it leads to fragile crystals or needles, which can be partly broken or totally detached from the parent crystals especially along structural anisotropic axis corresponding to weaker chemical bonds, thus leading to slower growing faces. When an activated mechanism is involved such as a secondary surface nucleation, it is no longer possible to obtain a steady state. Therefore, the crystal number, size and habit vary significantly with time, leading to troubles in the downstream processing operations and to modifications of the final solid-specific properties.

These results provide valuable information on the unique crystallization mechanisms of acicular crystals, and show that it is important to know these threshold and critical values when running a crystallizer in order to obtain easy-to-handle crystals.

PACS: 81.10.Aj; 81.10.Dn; 78.30.Jw

Keywords: A1. Crystal morphology; A2. Growth from solutions; B1. Organic compounds

1. Introduction

Many organic molecules exhibit anisotropic structural properties in their crystalline form, which gives rise to acicular or needle-like crystals. In the chemical and pharmaceutical industry, crystallization from solution is used as a separation technique, and this crystal habit is usually not desirable, especially when the internal length-to-width ratio is high, as it will lead to problems in downstream processes (filtration, drying, storage, handling, etc.).

A better understanding of the mechanisms of nucleation and growth of these needle-like crystals will therefore lead to better control of crystallization processes. In the literature, papers on molecular modeling of these needle-like crystals [1–3] suggest that in the case of needle-like crystals, there is no slow-growing face in the needle direction. Practical aspects have been also studied for a few years now in our different research teams [4–6].

In this contribution, we present an experimental investigation of the growth of four different organic molecules produced at industrial scale with a view to understand the crystallization mechanism of acicular

*Corresponding author. Tel.: +33 6 6292 2866; fax: +33 4 9141 8916.
E-mail address: veesler@crmcn.univ-mrs.fr (S. Veesler).
[1]Laboratory associated to the Universities Aix-Marseille II and III.

0022-0248/$ - see front matter © 2007 Elsevier B.V. All rights reserved.
doi:10.1016/j.jcrysgro.2007.10.006

crystals from the molecular to the macroscopic scales. For all organic crystals studied in this article, layer-by-layer growth of the lateral faces is very slow and clearly, as soon as supersaturation is high enough, there is competition between growth and activated secondary nucleation. These investigations show that crystals are agglomerated with the same crystallographic orientation for the individual constituents, as observed by optical microscopy, scanning electron microscope (SEM) and atomic force microscopy (AFM); this is explained by regular over- and inter-growths as in the case of twinning. And when supersaturation is even higher, nucleation is fast and random. These results provide valuable information on the unique crystallization mechanisms of acicular crystals, and show that it is important to know these threshold and critical values when running a crystallizer in order to obtain easy-to-handle crystals.

2. Materials and methods

2.1. Materials

The four organic molecules studied were:

(i) Irbesartan ($C_{25}H_{28}N_6O$), an active pharmaceutical ingredient crystallized in 2-propanol and used by Sanofi-Aventis in the treatment of hypertension;
(ii) Product 2 (for the sake of confidentiality), an organic molecule exhibiting an alkyl cycle with one polar chemical group: this molecule crystallizes in its industrial solvent;
(iii) Hydroquinone ($C_6H_6O_2$), which crystallizes in water in the presence of an additive used at industrial scale to specifically reduce growth along the length axis of the needle;
(iv) Product 4 (for the sake of confidentiality) known to exhibit only needle-like habit whatever the solvent used.

Structural data for the first three molecules are presented in Table 1.

Table 1
Structural data

	Irbesartan phase A[a]	Product 2	Hydroquinone phase α[a]
a (Å)	37.09	4.922	38.46
b (Å)	37.09	15.714	38.46
c (Å)	9.65	8.174	5.65
α (°)	90	90	90
β (°)	90	104.6	90
γ (°)	120	90	120

[a]Interestingly, Irbesartan phase A and hydroquinone phase α have the same space group R-3.

2.2. Solid Characterization

Crystals were observed under a (SEM; JEOL 6320F). SEM photographs clearly show the needle-like crystal habit for the four systems studied (Fig. 1). Crystals of Irbesartan phase A were also observed by AFM using a Digital Nanoscope III atomic force microscope equipped with a 12 μm scanner. Images were collected in tapping mode using oxide-sharpened Si_3N_4 cantilever tips (nanoprobe^{TM}).

2.3. Crystal preparation

Irbesartan and Product 4 crystals were grown in quiescent solutions (2 mL) at known concentrations, under optical microscope (Nikon, Diaphot), at given temperatures, using the experimental setup previously described [7].

Product 2 and hydroquinone crystals were obtained from isothermal crystallization in 2.5 L stirred vessels in semi-batch and continuous operations, respectively. Experimental procedures can be found in the following references [5,6,8]. The supersaturation is defined as $\beta = C/C_e$, with C and C_e are the concentration and solubility of the organic molecule.

3. Results and discussion

As shown in Fig. 1, all the crystals present a needle-like habit, which is due to a strong structural anisotropy along the *z*-axis for Irbesartan and hydroquinone, and *x*-axis for Product 2 (see Table 1). This was confirmed by molecular modeling for Irbesartan [4] and Product 2 [9]. Product 4 structure has not yet been determined.

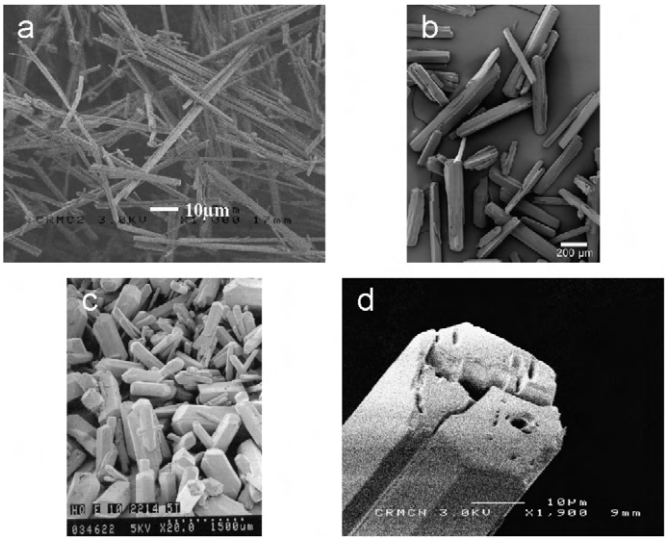

Fig. 1. Needle-like crystals observed by SEM: (a) Irbesartan phase A, (b) Product 2, (c) hydroquinone phase α and (d) Product 4.

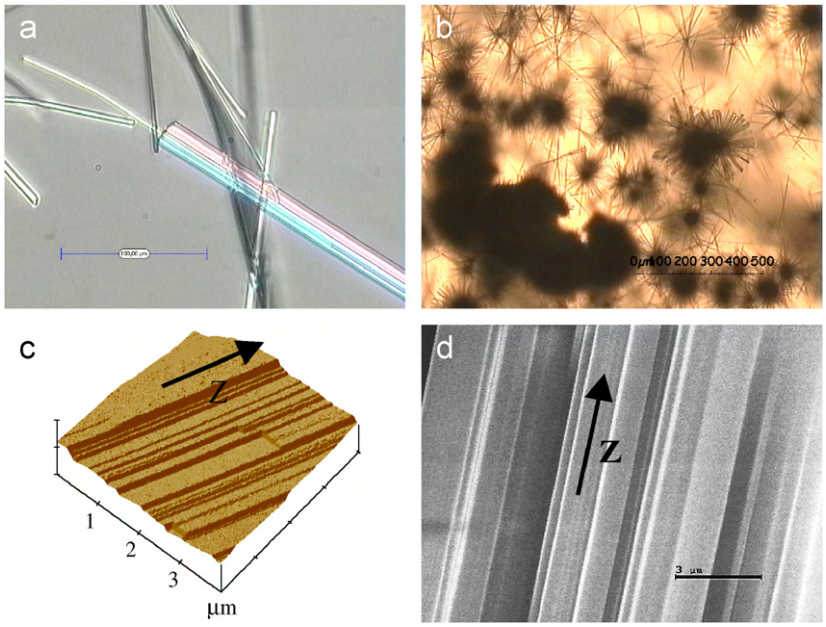

Fig. 2. Crystals of Irbesartan phase A: (a, b) optical-microscopy images, (c) AFM image and (d) SEM image.

3.1. Crystallization of Irbesartan in stagnant conditions

The experiments show that in all the temperature and supersaturation ranges, 2–20 °C and 3–10, respectively, crystals obtained (Fig. 2a, c and d) have a needle-like habit, composed by crystalline agglomerates.[2] Moreover, when supersaturation is too low, top faces do not grow. Supersaturation must exceed a threshold value in order for growth of the crystal in the needle direction (crystallographic z-axis) to be observed. The width of this dead zone is a function of the temperature and increases when the temperature decreases. The growth rate of the needle increases with increasing supersaturation up to a critical supersaturation (a second threshold) from which activated secondary nucleation appears, leading to a random nucleation of needles (Fig. 2b).

In the growth zone, below the critical supersaturation (second threshold), AFM observations clearly indicate that the agglomerate is composed of few needle-like crystals of different sizes but with the same crystallographic orientation along the z-crystallographic axis (Fig. 2c and d).

3.2. Crystallization of Product 2 and hydroquinone in isothermal stirred tank

Crystallizations in stirred crystallizers were studied for the two other systems, Product 2 and hydroquinone.

[2]Usually the term agglomeration is used for a two-step process: encounter and association between particles suspended in solution, while in this article, the term agglomerate is used to qualify polycrystallinity with no assumption on the mechanism of formation.

3.2.1. Product 2

In the case of Product 2, crystallizations were realized in semi-batch operations, supersaturation was increased by feeding the crystallizer with a hot, undersaturated and clear solution. Moreover, the crystallizer was initially seeded with well-defined crystals in order to study activated secondary nucleation and crystal growth. Supersaturation was measured during the experiment by HPLC measurement and resulted in the profile given in Fig. 3. When feeding starts (at time 0), supersaturation begins to rise. Until supersaturation reaches 1.98, only growth of seed crystals is observed, mainly for the lateral faces. Impurities from the industrial solvent slow down the growth of the terminal faces (Fig. 4a). It is noteworthy that as in the case of Irbesartan (Fig. 2), we do not observe growth of a single crystal but a polycrystalline growth. Then, supersaturation in the crystallizer reaches a maximum of 1.98, a threshold value (see supersaturation profile in Fig. 3). At this value, activated surface secondary nucleation starts creating fine needle crystals (secondary nuclei) with a longer length-to-width ratio than seed crystals (Fig. 4b). Crystals are composed of a few needle-like crystals of different sizes but with the same crystallographic orientation along the x-crystallographic axis (Fig. 4c).

Moreover, in unseeded semi-batch experiments, when greater supersaturations are reached up to 2.8, crystals showing random agglomeration are observed due to fast primary nucleation (Fig. 4d) as in the case of Irbesartan phase A (Fig. 2b).

3.2.2. Hydroquinone

Preliminary batch-seeded crystallization was performed. For continuous isothermal crystallization, first a hot undersaturated solution was fed in, then crystals were

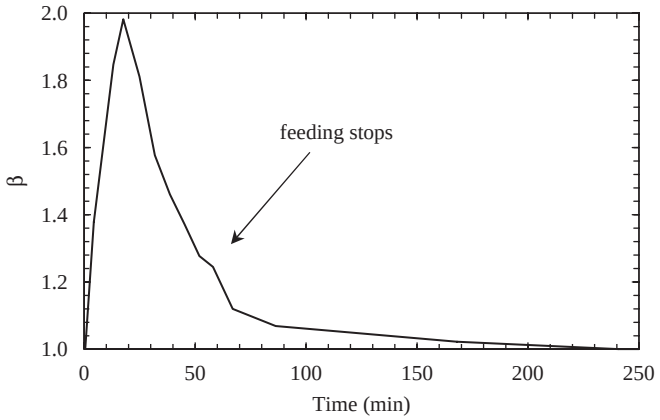

Fig. 3. Supersaturation profile of seeded semi-batch crystallization of Product 2.

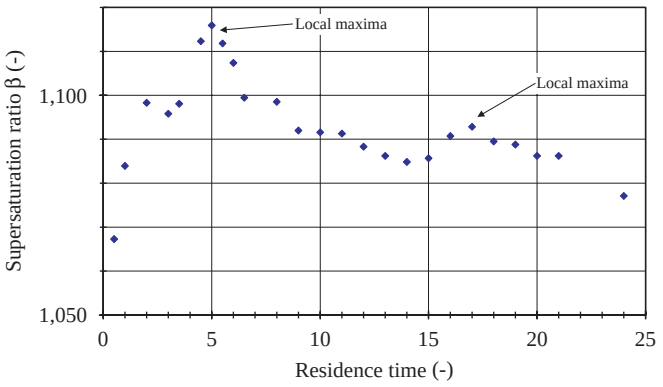

Fig. 5. Supersaturation profile in suspension of continuous crystallization of hydroquinone.

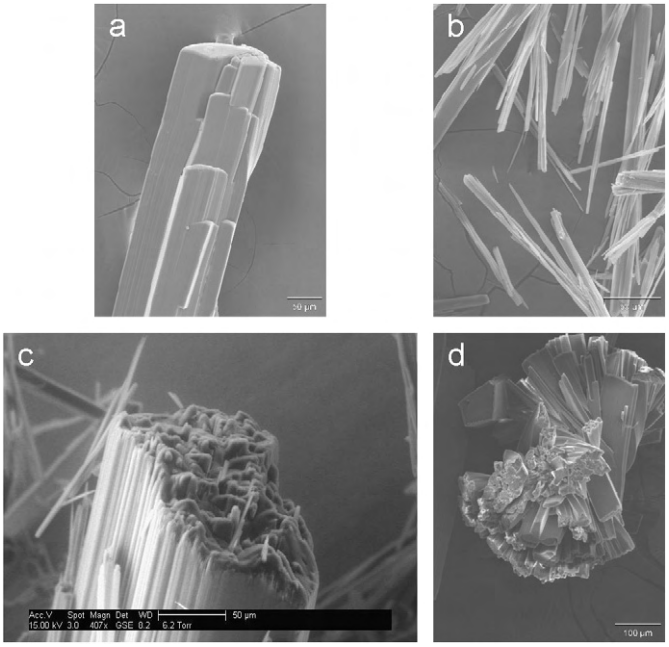

Fig. 4. SEM pictures of Product 2 crystals withdrawn (a) before threshold value at the beginning of the experiment, (b, c) after threshold value—respectively fine and seed crystals and (d) at higher supersaturation.

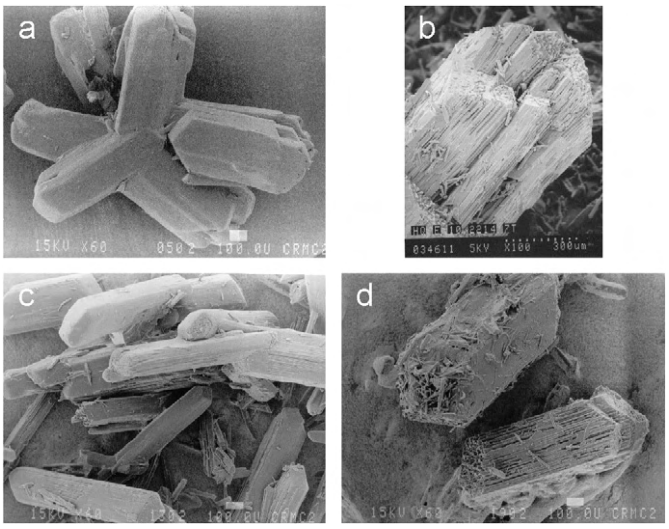

Fig. 6. SEM pictures of hydroquinone withdrawn at different residence times during a continuous isothermal crystallization—(a) reduced time = 5: before first burst of nuclei, (b) reduced time = 7: after first burst of nuclei, (c) reduced time = 13: before second burst of nuclei and (d) reduced time = 19: after second burst of nuclei.

nucleated and developed after which the suspension was withdrawn automatically to maintain the level of the reactor and immediately filtered. The solute concentration was measured regularly by a potentiometry analysis. Thus, the supersaturation was calculated from the knowledge of the solubility. After washing the crystals in acetone and vacuum drying, the crystals were weighed and measured [10] (image analysis) and observed under SEM.

Fig. 5 illustrates the supersaturation profile during one typical run. For 20 residence times, supersaturation did not reach a constant level, as normally expected. It showed two local maxima for the sixth and the seventeenth residence times. By coupling the mass balance and the crystal size distribution measurements, it was possible to evaluate the total number of crystals. This number decreased with an increase in supersaturation, and suddenly rose after a supersaturation maximum. These significant bursts of nuclei were visible to the naked eye. Before and after each supersaturation maximum, the mean dimensions of the crystals, respectively, showed a significant rise and fall. The evolution of the length-to-width ratio around the first supersaturation maximum was monitored [8]. Crystals nucleated and grown before this maximum were quite thick and exhibited a rod-like habit. Conversely, most of the crystals which were nucleated and grown after this maximum had a 40% higher length-to-width ratio leading to a needle-like habit (see Fig. 11 in Ref. [8]). Moreover, it was very instructive to observe how the appearance of the crystal surface evolved. During the first hours of the continuous operation, crystal surfaces were very smooth (see Fig. 6a). With the increase in supersaturation, crystals appeared to be more and more twinned. After the first maximum, the surfaces were rougher. On SEM

observations, the crystals were composed of numerous needle-like crystals with the same crystallographic orientation along the *z*-crystallographic axis (see Fig. 6b). Nevertheless, progressively with time, the surface appeared smoother (see Fig. 6c). A second increase in supersaturation followed by a second burst of nuclei was observed. Contrarily to the usual continuous operation, an unsteady state lasted throughout the run (20 h) although a steady state was expected after only 4 h. Lastly, whatever the operating conditions tested in terms of stirring rate and solid concentration, an irregular unsteady state was always observed, including one or two local maxima of supersaturation corresponding to thresholds where surface-activated secondary nucleation events started. Modifications in crystal surface appearance were systematically observed at different levels of supersaturation.

3.3. Discussion

In the case of Irbesartan, growth of the lateral faces was not observed under these conditions, meaning that the threshold supersaturation (from which growth is observable) of these faces is higher than the critical supersaturation for secondary nucleation. Thus, layer-by-layer growth of the lateral faces is more difficult than nucleation, meaning that surface-activated secondary nucleation is easier than growth. However, from AFM experiments (Fig. 2c), it can be assumed that the thickness of the acicular crystals is the result of agglomeration of several single needle-crystals. This agglomeration mechanism is not known but we can speak of regular over- and inter-growths, and as in the case of twinned crystals, two mechanisms need to be considered:

- *Synosis*: one individual nucleates, grows and deposits itself by one of its natural face on a face of a second already existing individual, in a proper crystallographic orientation according to the laws of regularity [11].
- *Faulted two-dimensional (2D) nucleation on the original composition plane*: the island is put on a twin orientation on the face of the original composition plane and grows to give the twin. Twins appear, once a threshold supersaturation has been exceeded [12,13].

The observation of reentrant angles in Fig. 7 confirms the assumption of twinning; this effect is commonly observed for contact twins and named as the reentrant corner effect.

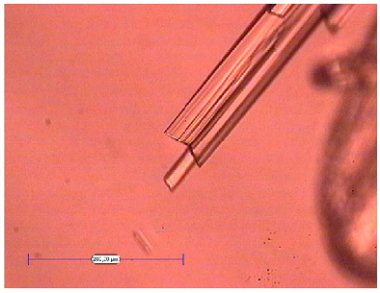

Fig. 7. Optical-microscopy image of needle-like crystal of Product 4.

The crystallization of Irbesartan and Product 4 were observed for individual crystals, which are giving information on microscopic growth mechanisms. Experiments for Product 2 and hydroquinone were performed in stirred vessels, providing macroscopic information for a population of crystals on the overall growth rate; similar experiments were carried-out on β-cyclodextrin [14]. However, whether one looks at the results from the microscopic or macroscopic scale experiments, similar nucleation and growth mechanisms of acicular crystals are observed. The crystallization mechanisms of Product 2 crystals are probably the same as for Irbesartan form A crystals described previously. However, the growth dead zone at lower supersaturation is not observed for Product 2, probably because the semi-batch crystallizations performed here do not provide enough information. In these experiments, at lower supersaturation, overall growth of crystals is regular and smooth but polycrystalline (see SEM pictures in Fig. 4a). At higher supersaturation, the growth mechanism is different and 2D nuclei can form onto crystal surfaces. Once formed, these nuclei detach and either (i) dissolve or grow inside the solution depending on their size, or (ii) grow on the surface of the parent crystal (synosis mechanism). Moreover, new nuclei can form on these still-growing surface needles giving an irregular appearance to seed crystals (faulted 2D nucleation).

The key parameter of these changes in behavior detected during the continuous crystallization of hydroquinone is the competition between growth and surface-activated secondary nucleation mechanisms. When the crystals came from a seeded batch operation, at low supersaturation levels, they exhibited a very smooth surface. The growth of the lateral surfaces was slow. The kinetics of attrition was poor and the total number of crystals decreased with time; consumption of solute by growth was thus less and less able to compensate for solute feeding. Supersaturation increased until a threshold was reached, leading to a burst of nuclei by a surface-activated secondary nucleation. On this emerging population, the lateral surfaces were striped along the needle direction and the secondary nucleation was more intense. This rough surface appearance was also observed on crystals produced during semi-batch experiments performed at higher level of supersaturation than continuous operations [10]. The kinetic of the secondary nucleation is then linked to the crystals surface appearance.

For all organic crystals studied in this article, layer-by-layer growth of the lateral faces is very slow and clearly, as soon as the supersaturation is high enough, there is competition between growth and surface-activated secondary nucleation. Moreover, at high supersaturation levels, surface-activated secondary nucleation and 2D nucleation, or the ''Birth and Spread'' growth mechanism, are closely linked. This gives rise to pseudo-twinned crystals composed of several needle individuals aligned along a crystallographic axis.

4. Conclusion

In this contribution, we present results for four different organic molecules, produced at industrial scale, crystallizing in needle-like habits. As supersaturation increases, several growth and nucleation mechanisms can be observed.

Experiments on Irbesartan show that at first, top faces do not grow at lower supersaturations (dead zone). Then, after a threshold value has been reached, growth starts and above a critical value, surface-activated secondary nucleation prevails.

The usual hypothesis, namely the crystallization mechanisms and consequently their kinetics remain constant during a continuous process can no longer be assumed, especially if the surface appearance of the faces shows modifications. In the case of hydroquinone, an increase in the level of supersaturations led to a change in surface appearance: thus, a surface-activated secondary nucleation linked to the surface appearance develops.

For all organic crystals studied in this article, layer-by-layer growth of the lateral faces is very slow and clearly, as soon as the supersaturation is high enough, there is competition between growth and surface-activated secondary nucleation.

This gives rise to pseudo-twinned crystals composed of several needle individuals aligned along a crystallographic axis as observed by optical microscopy, SEM and AFM; this is explained by regular over- and inter-growths as in the case of twinning. And when supersaturation is even higher, energy supplied to the system is high enough for nucleation to be fast and random.

In an industrial continuous crystallization, the rapid growth of needle-like crystals is to be avoided as it leads to fragile crystals or needles, which can be partly broken or totally detached from the parent crystals especially along structural anisotropic axis corresponding to weaker chemical bonds, thus leading to slower growing faces. When an activated mechanism is involved such as a secondary surface nucleation, it is no longer possible to obtain a steady state. Therefore, the crystal number, size and habit vary significantly with time, leading to troubles in the downstream processing operations and to modifications of the final solid-specific properties.

These results provide valuable information on the unique crystallization mechanisms of acicular crystals, and show that it is important to know these threshold and critical values when running a crystallizer in order to obtain easy-to-handle crystals.

Acknowledgments

The authors are indebted to Sanofi-Aventis, Arkema and Rhodia chemical companies for their financial supports for funding projects and for providing the industrial chemical compounds for the studies. We thank Mrs. M. Sweetko for English revision.

References

[1] H.M. Cuppen, A.R.T. Van Eerd, H. Meekes, Crystal Growth Des. 4 (2004) 989.
[2] H.M. Cuppen, G. Beurskens, S. Kozuka, K. Tsukamoto, J.M.M. Smits, R. De Gelder, R.F.P. Grimbergen, H. Meekes, Crystal Growth Des., 2005.
[3] D. Winn, M.F. Doherty, AIChE J. 44 (1998) 2501.
[4] P. Taulelle, J.P. Astier, C. Hoff, G. Pèpe, S. Veesler, Chem. Eng. Technol. 29 (2006) 239.
[5] F. Puel, G. Fevotte, J.P. Klein, Chem. Eng. Sci. 58 (2003) 3729.
[6] E. Verdurand, C. Bebon, D. Colson, J.-P. Klein, A.-F. Blandin, J.-M. Bossoutrot, J. Crystal Growth 275 (2005) e1363.
[7] S. Veesler, L. Lafferrere, E. Garcia, C. Hoff, Org. Proc. Res. Dev. 7 (2003) 983.
[8] F. Puel, P. Marchal, J.P. Klein, Trans. IChemE Part A 75 (1997) 193.
[9] E. Verdurand, Etude expérimentale et modélization de la nucléation secondaire lors de la crystallization d'un produit organique, Université Claude Bernard Lyon 1, 2004.
[10] F. Puel, Bilan de population pour deux tailles caractéristiques de particules: application à la crystallization de l'hydroquinone, UCB Lyon 1, 1994.
[11] G. Friedel, Leçons de cristallographie, Nancy, Paris, 1926.
[12] D. Aquilano, G. Sgualdino, in: N. Garti, K. Sato (Eds.), Crystallization Processes in Fats and Lipid Systems, Marcel Dekker, Inc., New York, 2001, pp. 1–51.
[13] R. Kern, Bull. Soc. Fr. Miner. Crist. LXXXIV (1961) 292.
[14] M. Kohl, F. Puel, J.P. Klein, C. Hoff, O. Monnier, J. Crystal Growth 270 (2004) 633.